

# The Connection from Cortical Area V1 to V5: A Light and Electron Microscopic Study

John C. Anderson,<sup>1</sup> Tom Binzegger,<sup>1</sup> Kevan A. C. Martin,<sup>1</sup> and K. S. Rockland<sup>2</sup>

<sup>1</sup>Institute for Neuroinformatics, 8057 Zürich, Switzerland, and <sup>2</sup>University of Iowa Hospitals and Clinics, Iowa City, Iowa 52242

Area V5 (middle temporal) in the superior temporal sulcus of macaque receives a direct projection from the primary visual cortex (V1). By injecting anterograde tracers (biotinylated dextran and *Phaseolus vulgaris* lectin) into V1, we have examined the synaptic boutons that they form in V5 in the electron microscope. Nearly 80% of the target cells in V5 were spiny (excitatory). The boutons formed asymmetric (Gray's type 1) synapses with spines (54%), dendrites (33%), and somata (13%). All somatic targets and some (26%) of the target dendritic shafts showed features characteristic of smooth (inhibitory) cells. Each bouton formed, on average, 1.7 synapses. The larger boutons formed multiple synapses with the same neuron

and completely enveloped the entire spine head. On most dendritic shafts and all somata the postsynaptic density *en face* was disk-shaped but in about half the cases the reconstructed postsynaptic densities of synapses on spines appeared as complete or partial annuli. Even in the zones of densest innervation only 3% of the asymmetric synapses were formed by the labeled boutons. Although the V1 projection forms only a small minority of synapses in V5, its effect could be considerably amplified by local circuits in V5, in a way analogous to the amplification of the small thalamic input to area V1.

**Key words:** visual cortex; area MT; corticocortical; synapse morphology; postsynaptic target; 3-D reconstruction

The best-studied extrastriate area is that first discovered by Zeki (1969), who used anatomical methods to define an area in the posterior bank of the superior temporal sulcus in macaque monkey that received an input from area 17. The homologous area in the new-world monkey is the middle temporal area (MT) (Allman and Kaas, 1971). From the earliest recordings, it was evident that the neurons of this area, now called MT or V5, were particularly sensitive to the direction and velocity of motion of the stimulus (Dubner and Zeki, 1971).

There are both direct and indirect projections from V1 to area V5 (Zeki, 1969; Ungerleider and Mishkin, 1979; Maunsell and Van Essen, 1983; Fries et al., 1985). The neurons that project directly from V1 have been identified as spiny stellates and pyramidal cells in layer 4B and large pyramidal cells in upper layer 6 (Lund et al., 1975; Shipp and Zeki, 1989). Their afferent axons form large boutons in a patchy distribution in layers 3, 4, and 6 of V5 (Rockland, 1989, 1995). The receptive fields of the V1 neurons that project to V5 have also been studied. The projecting neurons were identified by antidromically activating them from V5 (Movshon and Newsome, 1996). They had fast-conducting axons and all were binocular, complex cells, with high-contrast sensitivity and contrast-independent direction preferences. They responded at least as well to short stimuli as to long stimuli. Such complex cells are referred to as special (Palmer and Rosenquist, 1974) and have the largest receptive fields, the highest velocity preference, and the highest spontaneity of striate

cortical cells (Gilbert, 1977). This degree of uniformity in physiological properties seems to indicate that MT uses this output from V1 for further stages of specific processing. Movshon and Newsome (1996) suggested that these V1 neurons form the first stage of motion processing, in which the motion of the individual components of a pattern is extracted (Adelson and Movshon, 1982; Movshon and Newsome, 1984). The second stage occurs outside V1, in areas such as V2 and V5, where the motion of the entire pattern is computed.

If the V1 output to V5 is blocked, by making lesions or cooling V1 or blocking the magnocellular pathway, some activity persists in V5, but it is greatly diminished from normal. Although these experiments do not distinguish between the direct and indirect projection from V1 to V5, it is likely that the output from V1 is significant for V5. Anatomically, however, the picture is unclear. As yet there are not even qualitative estimates of the numbers of synapses involved in the V1 to V5 projections. In the present study we assessed the synaptic connections formed in V5 by the V1 projection neurons. Although the manner of connection of the V1 afferents to neurons in V5 was morphologically distinct, quantitatively they formed only a few percent of the synapses within their major termination zones in V5.

## MATERIALS AND METHODS

The materials examined in this study were obtained from two adult *Macaca mulatta* monkeys in the laboratory of K.S.R. (University of Iowa Hospitals and Clinics). The monkeys were prepared for surgery with a premedication of ketamine (11 mg/kg). Surgery was performed under deep anesthesia induced by intravenous delivery of Nembutal (25 mg/kg) and supplemented as required. All procedures were performed under sterile conditions in accordance with institutional and federal guidelines as specified in approved Animal Care and Use Research Forms.

One animal received a single microinjection of 10% biotinylated dextran amine (BDA) (Molecular Probes, Eugene, OR) in 0.0125 M PBS into cortical area V1. The second animal received a similar microinjection of BDA and a second injection of 2.5% *Phaseolus vulgaris* leucoag-

Received June 23, 1998; revised Aug. 27, 1998; accepted Sept. 14, 1998.

This work was supported by a Schweizer Schwerpunkt Programme Swiss National Science Foundation grant to Professor R. J. Douglas and K.A.C.M. and by National Institute of Mental Health/National Science Foundation Grants MH 53598 and IBN 9421970 to K.S.R. We are grateful to Professors W. T. Newsome and M. N. Shadlen for their critical reading of an earlier draft of this manuscript.

Correspondence should be addressed to John C. Anderson and Kevan A. C. Martin, University/ETH Zürich, Winterthurerstrasse 150, 8057 Zürich, Switzerland. Copyright © 1998 Society for Neuroscience 0270-6474/98/1810525-16\$05.00/0

glutinen (PHA-L) (Vector Laboratories, Burlingame, CA) in 10 mM phosphate buffer (PB) (see Fig. 1). Each injection was  $\sim 0.5 \mu\text{l}$ . After an 18 d survival period the animals were anesthetized and perfused transcardially with a solution of paraformaldehyde (4%) and glutaraldehyde (0.25%) in saline, followed by sucrose solutions of 5, 10, and 15% in 0.1 M PB. After the brain was removed from the skull, a block of tissue ( $\sim 15$  mm in dorsoventral extent) was trimmed through the superior temporal sulcus (STS) intended to include cortical area V5 or MT. The selected block of cortex was bisected and vibratome-sectioned in the horizontal plane at  $50 \mu\text{m}$ . Sections were collected in 20% sucrose in PB and kept overnight in the refrigerator. Sections were then immersed in liquid nitrogen for rapid freezing as a way of promoting penetration. After thawing, the sections were processed according to a Vector ABC kit (Elite) protocol to visualize labeled axons. We used 3, 3'-diaminobenzidine tetrahydrochloride (DAB) to reveal peroxidase activity. For tissue injected with BDA, this followed 24 hr in ABC solution. For PHA-L-injected tissue, this followed 2 d in anti-PHA-L (1:2000) and repeated 70 min steps through secondary antibody and ABC solutions. Selected sections were treated with a 0.5–1% osmium tetroxide solution in 0.1 M PB. Dehydration through an ascending series of alcohols (including 1% uranyl acetate in the 70% alcohol) and propylene oxide preceded flat mounting in Durcupan (Fluka ACM, Buchs, Switzerland) onto glass slides.

The labeled axons were reconstructed by light microscopy. Regions of special interest were photographed and re-embedded for correlated electron microscopy (EM). Serial ultrathin sections were cut at 70 nm thickness and collected on Pioloform-coated single-slot copper grids. Labeled profiles were photographed at  $21,000\times$  magnification. The classification of synapses as symmetric or asymmetric was made on the basis of conventional criteria (Gray, 1959; Colonnier, 1968). The presence of reaction product in the presynaptic bouton obviously compromises the visibility of the presynaptic membrane. However, the unlabeled boutons in the adjacent neuropil indicated marked differences in the thickness of the postsynaptic density of symmetric and asymmetric synapses (see Fig. 4). This allowed us to make definitive classifications of the synapses formed by labeled boutons. Serial electron micrographs of labeled synaptic boutons were digitized and reconstructed using an in-house computer system (Trakem). From the digitized and reconstructed data, we measured structures such as postsynaptic specializations and bouton area. Trakem generates a series of wire frame profiles, which gives a three-dimensional (3-D) impression. The "object" can be rotated to offer different views of synapses. We enhanced this effect by fitting a skin to the digitized structure and then rendering the surface. The skin fitting used Nuages (B. Geiger, 1996), and the rendering used Geomview and Blue Moon Rendering Tools (L. Gritz).

To reconstruct and measure the area of postsynaptic densities of labeled boutons in 3-D, we developed our own computer software. A semiautomated process first grouped the serially sectioned components of synapses. The postsynaptic surface was represented as a 3-D grid that was created by interpolating points between the components. The area was measured by summing the areas of the triangles that appeared between the interpolated points. To represent the reconstructed synapses in two dimensions, we selected an appropriate plane on which to project each synapse.

We used the physical disector method of Sterio (1984) to obtain a stereological estimate of the percentage of labeled synapses in area MT. Serial ultrathin (70 nm) sections were cut and collected as above. Reference and look-up sections were separated by one intervening section. Each section was photographed in the EM at  $11,500\times$ . Only those synapses that appeared in the reference section but not in the look-up section were counted here.

## RESULTS

### Light microscope observations

Pressure injections of biotinylated dextran amine (one animal) or BDA and PHA-L (one animal) were made into the parafoveal representation in area 17 (V1) (Fig. 1). After processing, the injections were found to be 1–2 mm in diameter and confined to the gray matter. At one site the white matter was damaged by the injection needle itself. In area V5, labeled axons arborized in layers 3, 4, and 6. The lack of labeled cell bodies in extrastriate cortex was taken as evidence that the transport was anterograde only. The largest diameter ( $3 \mu\text{m}$ ) axons showed the label only at

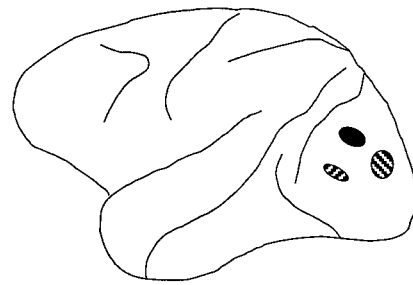


**Figure 1.** Summary schematic of macaque brain showing position of three injections of neuronal tracers (2 of BDA and 1 of PHA-L) into primary visual cortex, area V1, of two animals.

the cut ends and not in the middle of the section. Presumably this is because the avidin complex could not penetrate the thick myelin sheath surrounding the labeled axons, despite the freeze-thaw procedure. These heavily myelinated fibers, originating from V1, arose from the white matter and branched to produce collaterals of decreasing diameter as they ascended through the cortical layers. The smaller-diameter collaterals retained a myelin sheath, which was not so thick as to prevent penetration of the reagents. The axons appeared unmyelinated in the light microscope (LM) at the point where boutons formed. This was confirmed in the electron microscope. Long, uninterrupted lengths of very fine collaterals also criss-crossed the termination zones. The boutons formed by these fine collaterals were very small and infrequent ( $<1/100 \mu\text{m}$ ). The fine collaterals were not from a separate population of afferents, but branched from axons that bore large boutons. All boutons selected for this study were located in layers 4 and 6 of area V5.

Short strings of large boutons (up to  $3 \mu\text{m}$  diameter) of both *en passant* and *terminaux* morphology were gathered in local clusters. Some of these boutons formed close appositions with somata. From the LM views (Fig. 2A; see also Fig. 5A) we chose collaterals that formed clusters of boutons that were more or less parallel to the face of the section. This selection somewhat reduces the number of serial ultrathin sections from unmanageable to very large. Long lengths of collaterals, including the interbouton segments, were also traced through the serial ultrathin sections. We examined 86 boutons (32 from layer 6 and 54 from layer 4) in the electron microscope. Each bouton formed at least one asymmetric (Gray's type 1) synapse.

### Electron microscopy

#### Synapses formed with dendritic spines

Figure 2 illustrates a correlated LM and EM sample from labeled collaterals in layer 4. The reaction end-product was very intense in many of the boutons. Where this reaction end-product was most intense it produced "chatter" over the labeled regions in the ultrathin section. The heavy labeling made the details of the presynaptic structures difficult to see, but the synaptic cleft and the postsynaptic specialization were unaffected by the labeling. The synaptic vesicles and mitochondria within the bouton did not contain any significant deposit of reaction end-product. The labeled boutons were usually packed with mitochondria and round vesicles (Fig. 2B–E). Some of the boutons and parts of the axon contained vacuoles (e.g., Fig. 2C–E). These were clearly artifacts of the labeling process, because unlabeled structures in the adjacent neuropil were intact. Similar vacuoles have been reported with the use of wheat-germ agglutinin as a tracer (LeVay, 1986). Vacuoles might contribute to the distinctive size of boutons when

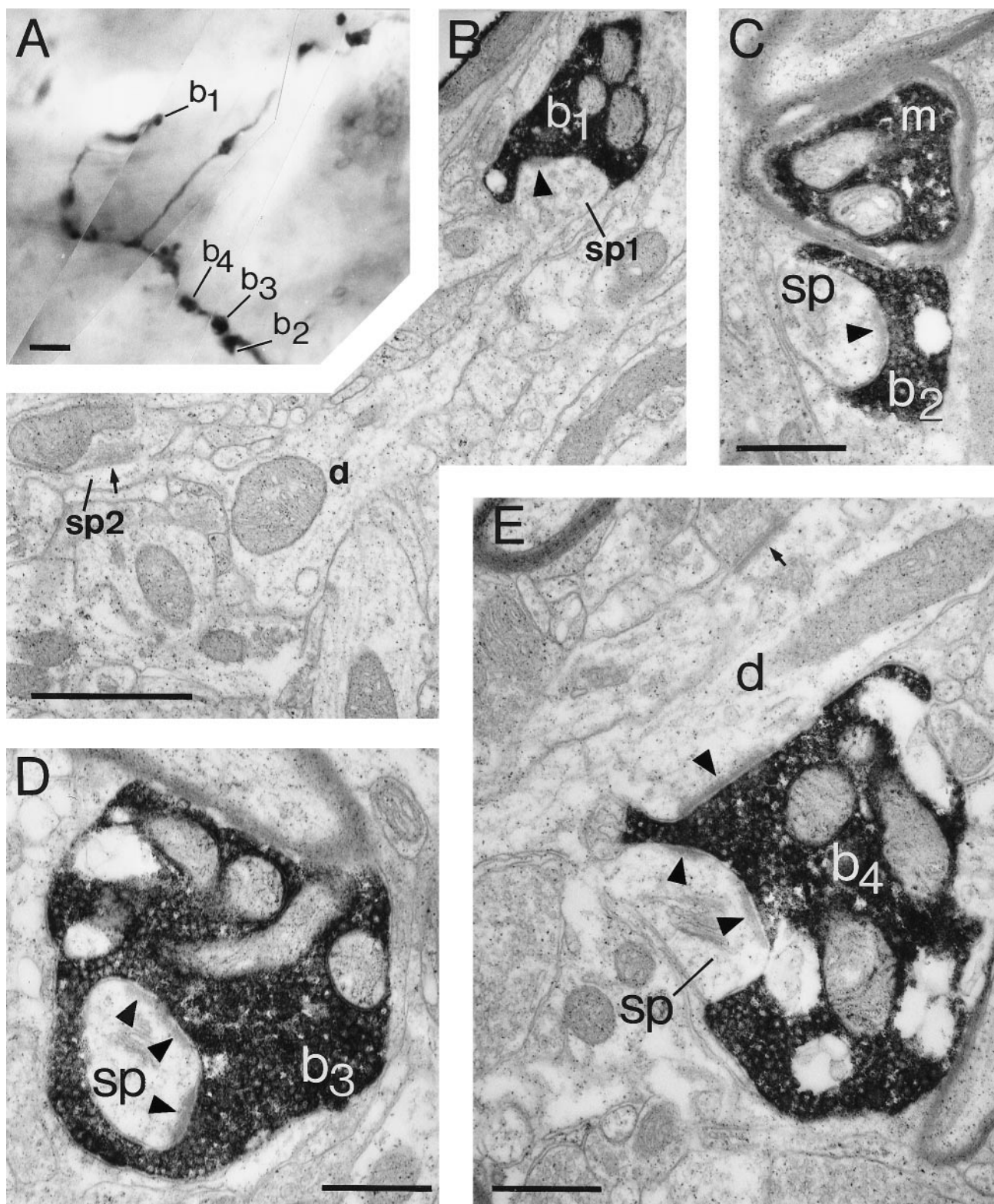


**Figure 2.** Correlated light and electron micrographs of BDA/PHA-L-labeled electron dense axon and boutons. *A*, Photomontage of an axon collateral located in lower layer 4 of area V5; b1, b2, b3, and b4 are selected boutons. The associated synapses of these boutons are shown in the following electron micrographs. *B*, Bouton b1 forms an asymmetric synapse (solid arrowhead) with a spine head (sp1) that can be traced back to the parent dendrite (*d*) in a single section. The dendrite produces a second spine (sp2), which receives an asymmetric synapse (small arrow) from an unidentified bouton. *C*, A myelinated axon collateral (*m*) gives rise to a bouton (b2) forming an asymmetric synapse (solid arrowhead) with a spine (*sp*). *D*, A large bouton (b3) packed with vesicles and mitochondria forms an asymmetric synapse (solid arrowheads) with a spine (*sp*). The spine profile has been completely embraced by the filled bouton. The postsynaptic density does not appear as a continuous structure but instead is perforated or complex. *E*, Another large bouton (b4) forms asymmetric synapses (solid arrowheads) with a spine (*sp*) and the shaft of a dendrite (*d*). The spine apparatus is clearly visible. The dendrite also forms an asymmetric synapse (small arrow) with an unidentified bouton. Scale bars: *A*, 10  $\mu\text{m}$ ; *B*, 1  $\mu\text{m}$ ; *C–E*, 0.5  $\mu\text{m}$ .

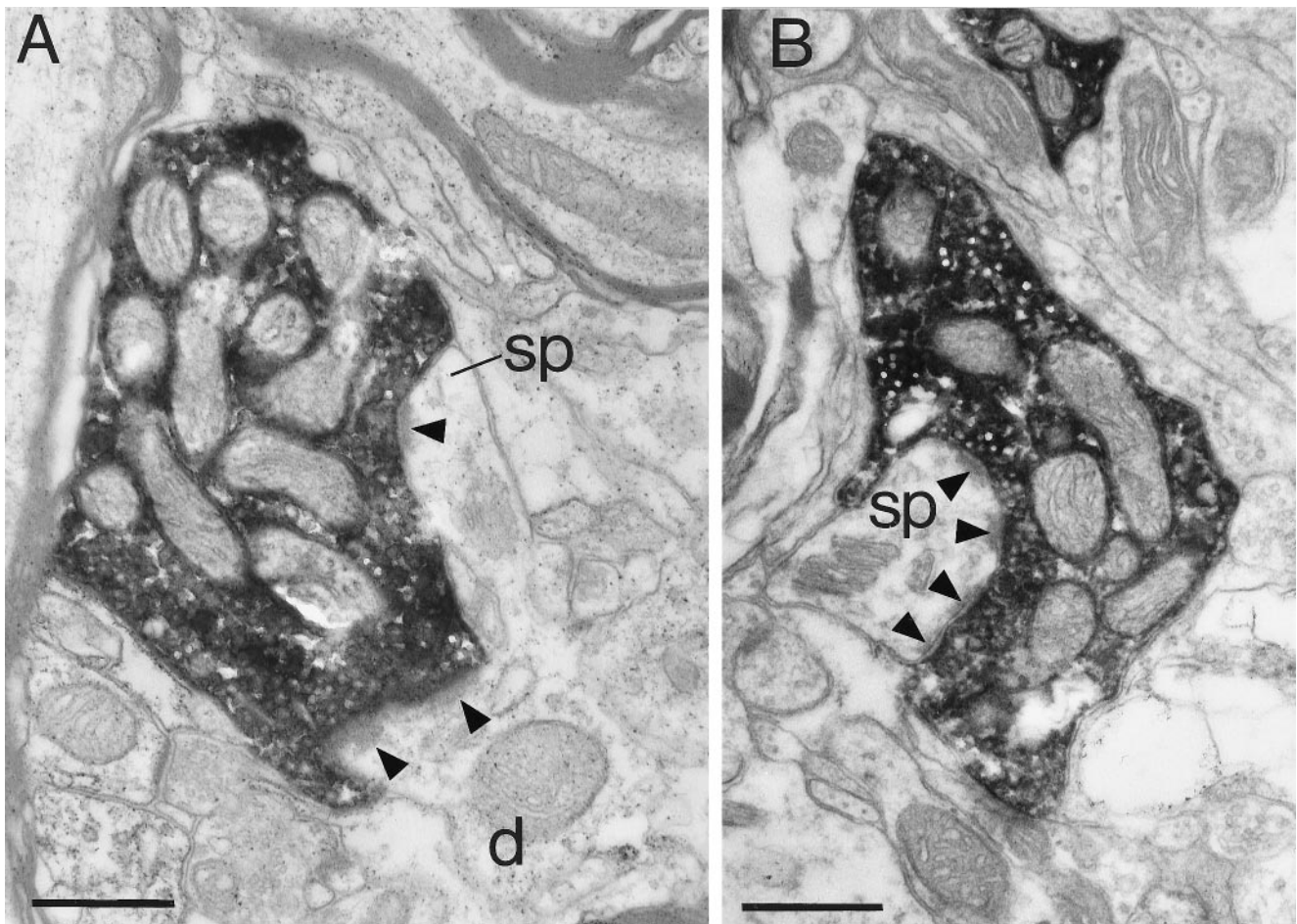


**Figure 3.** Electron micrographs of BDA/PHA-L-labeled boutons found in layer 6 of area V5. *A*, Bouton filled with mitochondria forming two asymmetric synapses (solid arrowheads) with the same target neuron. One of the targets is clearly a spine (*sp*; note the spine apparatus) that can be traced back to the parent dendrite (*d*). The second synapse forms on a region of the dendritic shaft that projects slightly into the neuropil. Serial section reconstruction showed this projection to be a sessile or “neckless” spine. *B*, A spine (*sp*) containing spine apparatus forms an asymmetric synapse with the labeled bouton, which shows a complex postsynaptic density (solid arrowheads) within the spine. Scale bars, 0.5  $\mu\text{m}$ .

viewed in an LM, although the largest boutons in our sample contained no vacuoles.

The collaterals that gave rise to strings of boutons were frequently myelinated, but not so strongly that the avidin complex could not penetrate (Fig. 2*A,C*). The boutons along the collaterals formed asymmetric (Gray’s type 1) synapses (Figs. 2, 3). The standard ultrastructural criteria, particularly spine apparatus (Peters et al., 1991) in conjunction with serial section reconstruction of the bouton and its target, helped to identify the target. Sometimes the spine neck could be traced back to the parent dendrite, either over several sections or occasionally in a single section (Figs. 2*B,E*, 3*A*). This was made possible because in some cases the spines had a relatively thick spine neck that was only a little smaller in cross section than the spine head. The majority of spines, unfortunately, could not be traced to their parent dendrites despite care being taken in collecting serial sections.

Some spine heads were actually embedded deep in the bouton itself (Fig. 2*D*) and in many cases the bouton wrapped around the spine head (Figs. 2*B,C,E*, 3*A,B*). Further detailed reconstructions are given below. The postsynaptic densities were not single entities but were frequently divided into a number of separate zones, as indicated in Figures 2*D* and 3*B*, *arrowheads*. The labeled bouton was the only source of asymmetric synapse to the spine. In

three cases the spine formed a second, symmetric (Gray’s type 2) synapse with an unlabeled bouton. When reconstructed, eight of the boutons that formed a synapse with a spine also formed synapses with the parent dendrite or a sessile spine from the parent dendrite. One bouton formed synapses with two spines and a dendritic shaft; all three targets belonged to the same neuron (b1 in Fig. 2*A,B*).

#### *Synapses formed with the shafts of dendrites*

Dendritic shafts were identified by their numerous mitochondria and microtubules, and in some cases by their projecting spines. Figure 4 illustrates the synapses formed with dendritic shafts. Figure 4*A* illustrates a bouton sampled from layer 4 that forms a synapse (*large, filled arrowhead*) with a large caliber dendrite (*d*) and a spine (*sp, large, filled arrowhead*). The dendrite forms numerous synapses from unlabeled boutons (*small and unfilled arrowheads*). The dendrite contained many large mitochondria, particularly in the dendritic varicosities or “beads.” The beads (one is evident in the Fig. 4*A*) were more evident in serial reconstruction. No spines emerged from the shaft. These features are all characteristic of the dendrites of smooth neurons (Somogyi et al., 1983; Peters and Saint Marie, 1984; Kisvárdy et al., 1985; Ahmed et al., 1997). Some of the adjacent unidentified

synapses on the same target dendrites were symmetric (Fig. 4A, *open arrowheads*), although the majority were asymmetric (Fig. 4A, *small, filled arrowheads*). Smaller-diameter dendrites with no symmetric synapses but otherwise similar features were also the targets of labeled boutons. One dendrite of small diameter formed a synapse with a labeled segment of axon. This contact was not anticipated, because at the LM level there was no suggestion of a bouton. Despite lengthy serial sections of axons, this was the only synapse discovered, indicating that such axonal synapses must be exceedingly rare.

The bouton illustrated in Figure 4B (sampled from layer 6) formed a synapse with a smooth beaded dendritic shaft similar to that described above (Fig. 4A). In the higher-power view of the synapse (Fig. 4C), the additional unlabeled boutons that form synapses with the dendrite were packed together. One formed symmetric synapses (*open arrowheads*), one formed asymmetric synapses (*small, filled arrowhead*). Approximately 26% of the dendritic shafts in V5 that formed synapses with the V1 afferents were of this smooth neuron type.

#### *Synapses formed with somata*

Neuronal somata in both layers 4 and 6 also formed synapses with V1 afferent boutons. Figure 5 illustrates a soma in layer 4 that forms synapses with four separate boutons (Fig. 5B, *b1–b4*) that arose from one myelinated axon collateral. Contacts between somata and the darkly labeled boutons of the V1 axons were easily visible at the LM level (Fig. 5A,B). The postsynaptic somata contained large, deeply invaginated nuclei, and the cytoplasm was packed with mitochondria (examples indicated by *arrows* in low-power electron micrograph in Fig. 5C) and rough endoplasmic reticulum. Crystalline inclusion bodies were sometimes found within the mitochondria of contacted somata (Fig. 5H). These have previously been seen within the mitochondria of Meynert cells in area V1 of monkey cortex (Chan-Palay et al., 1974). The Meynert cells project to V5 (Lund et al., 1975; Maunsell and Van Essen, 1983; Fries et al., 1985). All of the synapses formed with the soma by unlabeled boutons were asymmetric. However, the postsynaptic density of somatic synapses was far less prominent than those formed with spines and shafts. The ultrastructural features of the somata are characteristic of GABAergic smooth neurons (Peters and Saint Marie, 1984).

#### *Three-dimensional reconstructions of synapses*

One intriguing aspect of the large labeled boutons became evident when we reconstructed them and their synaptic targets more fully. Because the geometry might be of significance for the diffusion of transmitter to receptors from the presynaptic release sites (Uteshev and Pennefather, 1997; Rusakov and Kullmann, 1998a,b) we have made complete reconstructions of some boutons to illustrate the feature (Figs. 6, 7). The asymmetric synapses formed with spines were made by boutons that enveloped the spine head, which formed a virtual pocket within the volume of the bouton (Fig. 6A,B). Sometimes the bouton completely engulfed the spine head (Fig. 6C,D). Almost half (46%) of the spine heads in our sample were enveloped by the bouton. When synapses were formed, as these examples show, the synapse itself could be located at the tip of the spine or close to the point of penetration of the spine into the bouton, or both. The large bouton illustrated in Figure 7 formed synapses with four spines and a dendritic shaft. This exceptional bouton formed eight distinct synapses. The entire heads of two bulbous spines were almost completely enveloped by the bouton. The other two spines

were also less completely enveloped. The entire circumference of a dendritic shaft was enveloped by the bouton. It formed three synapses with the labeled bouton. The target dendrite was varicose, packed with mitochondria, and formed one other synapse with an unidentified bouton. It had no spines in the reconstructed section and most likely was a dendrite of a smooth neuron.

The detail of the postsynaptic membrane was sufficiently well preserved that we could reconstruct the complete postsynaptic surface of synapses. It became clear that different types of target formed synapses of different size and shape. The shape of the postsynaptic disk could vary because of perforations in the postsynaptic density (Peters et al., 1991). This results in a “complex” synapse. Figure 8 depicts the two-dimensional projection of the postsynaptic densities from the sample of complete 3-D reconstructions of the synapses. Postsynaptic densities in the form of annuli and horseshoe shapes were more frequent on spines. Dendritic shafts and somata in particular had the least perforated or complex postsynaptic densities. It was a matter of opinion whether the numerous, small synapses formed with somata were in fact one synapse, but because each synaptic site could be separated by up to seven sections they were considered to be individual sites. However, the arrangement of vesicles above these multi-synaptic sites was of a continuous dense cloud of vesicles. Sessile spines could form synapses with regular or complex postsynaptic densities.

The histogram of synaptic areas (Fig. 9) indicates that synapses made by the boutons contacting somata were the smallest: mean area  $0.031 \mu\text{m}^2$  (SEM = 0.008). Spine synapses were the largest on average ( $0.127 \mu\text{m}^2$ ; SEM = 0.011), and those with dendritic shafts were intermediate ( $0.071 \mu\text{m}^2$ ; SEM = 0.07). The synapse areas of the three groups are significantly different from each other ( $p = 0.01$ ; Wilcoxon paired rank test). Most synapses extended over only two or three sections; however, one bouton could provide up to five small synapses.

#### *Mitochondria in boutons*

Evidence is accumulating that because of their role in calcium metabolism, the mitochondria in axonal boutons may have a significant influence on the dynamics of synaptic transmission (Nicholls and Åkerman, 1982; Herrington et al., 1996; Tang and Zucker, 1997; Xu et al., 1997; Peng, 1998). We have thus fully reconstructed several boutons to examine the details of their mitochondrial contents more completely. These 3-D reconstructions indicated that the region adjacent to the synapse had the greatest accumulation of vesicles. Mitochondria of variable diameter filled out the remainder of the volume of the bouton. Up to 12 mitochondrial profiles, sometimes branched, could appear in any single ultrathin section. Three-dimensional reconstructions of mitochondria have rarely been made in such boutons, so the actual number of individual mitochondria is unknown. After reconstructing some of these structures (Fig. 10) we discovered that there was considerable variation in the organization of mitochondria. In some boutons the densely packed mitochondria were relatively short ( $0.5 \mu\text{m}$ ) and straight, and in others they formed continuous loops within the volume of the bouton (Fig. 10). Hence the same mitochondrion was sectioned many times in each ultrathin section. As the bouton volume increased, so the number of mitochondrial profiles increased, but not necessarily the total number of mitochondria. We could follow individual mitochondria as they streamed from the bouton into the axon [e.g., the mitochondria represented in *dark orange* and *pale green* (Fig. 10C,D)]. The reconstructions also showed that the mito-

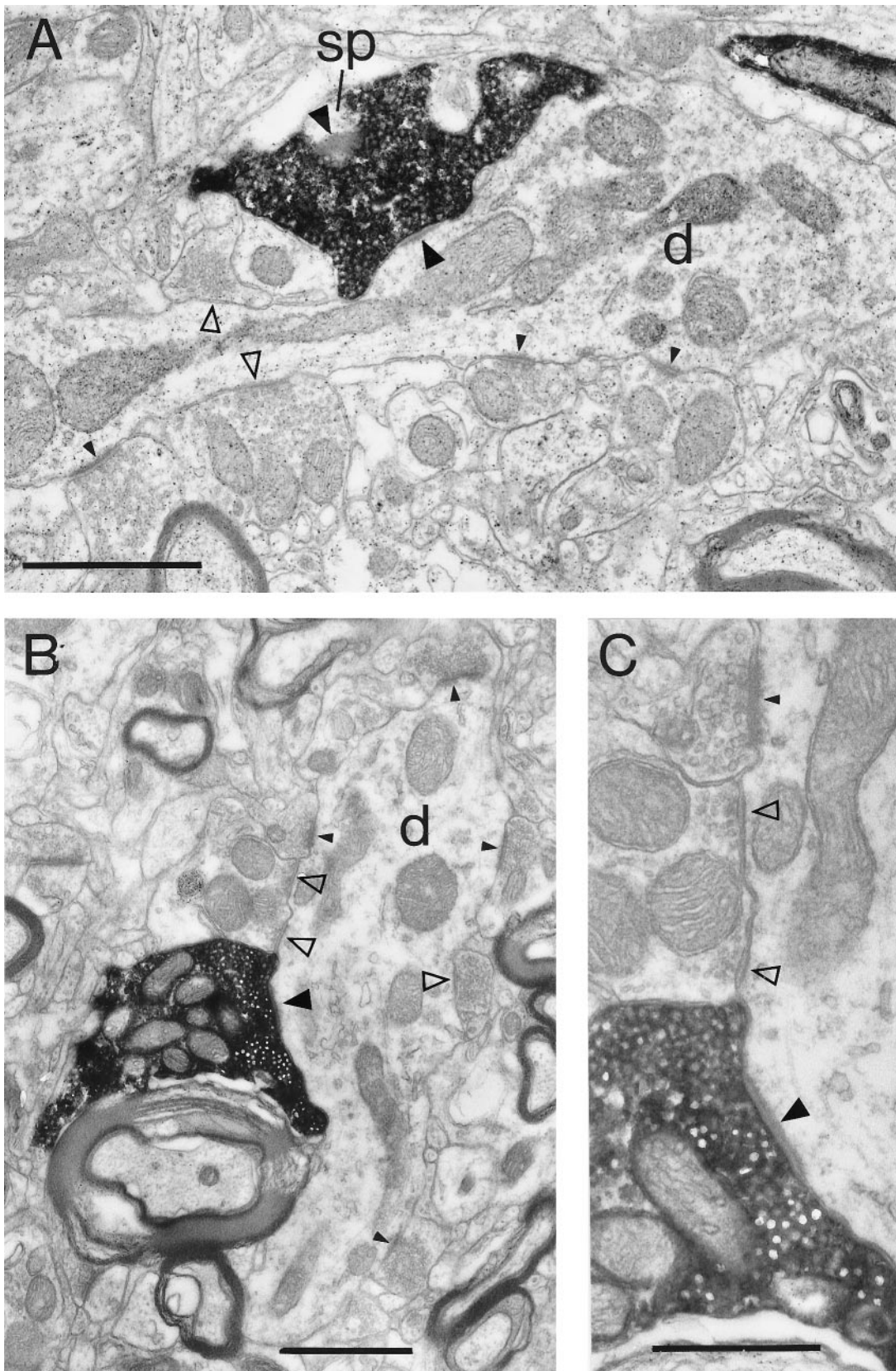


**Figure 4.** Electron micrographs of labeled synaptic boutons in contact with dendrites of smooth cells. *A*, Characteristically large bouton, filled with vesicles, located in lower layer 4 forms two asymmetric synapses (*large, solid arrowheads*), one with a dendrite (*d*) and the other with a spine (*sp*). The dendrite contains numerous mitochondria and forms many synapses of the symmetric (*open arrowheads*) and asymmetric (*small, solid arrowheads*) types with unidentified boutons. When the target dendrite was reconstructed over several serial sections, it became clear that the variations in diameter, which can be visible in the micrograph, were caused by a varicose or beaded morphology. These features are consistent with (*Figure legend continues*)

chondria accumulated at one side of the bouton, away from the synapses themselves. This space immediately around the synapses was filled with vesicles. Measurements in three fully reconstructed boutons revealed that the mitochondria occupied an average volume of  $0.57 \mu\text{m}^3$ , which was fully 22% of the entire average volume of the boutons. The total surface area of the mitochondria within a bouton was approximately equal to the surface area of the bouton.

#### *Targets of synapses*

Data from layers 4 and 6 were pooled because no significant differences between the two samples were observed. The principal synaptic targets of the V1 afferents were spines, which formed 54% of targets. Dendritic shafts formed a large proportion of targets (33%), about a quarter of which originated from smooth neurons. Somata, probably also of smooth neurons, formed the remaining 13% of targets (Fig. 11). Thus,  $\sim 78\%$  of the V1 afferent synapses were formed with spiny excitatory neurons in V5. Most boutons formed only one asymmetric synapse (Fig. 12). However, some formed two or more synapses, so that on average each V1 afferent bouton formed 1.7 synapses.

#### *Proportion of asymmetric synapses formed by V1 afferents in layer 4 of V5*

When sections were viewed in the LM it was clear that the labeled processes were not distributed evenly (Rockland, 1989) but formed zones of higher and lower density. From one monkey we selected two patches of particularly dense labeling within layer 4 for a stereological assessment by the unbiased “disector” method (Sterio, 1984) of the proportion of labeled synapses. This method entails the use of serial sections. Synapses appearing in the “reference” section but not in the “look-up” section are counted. We found that 2.7% (5 of 185) and 3.5% (3 of 85) of boutons with disappearing synapses (Sterio, 1984) were labeled. The area (micrometers squared) of all labeled and nonlabeled boutons with disappearing synapses ( $n = 270$ ) was measured. The size distribution of the unlabeled and labeled profiles was broad (Fig. 13). Labeled profiles did not occupy the lowest end of the distribution but were evident among the largest measured. In the same tissue we could assess labeled versus nonlabeled myelinated axon profiles. Labeled myelinated axons occurred with about the same frequency (2.8%) as labeled synapses. The largest diameter axons ( $\sim 2 \mu\text{m}$ ) in layer 4 were both labeled and nonlabeled. All of the large-diameter axons were covered with a myelin sheath. The wall of the myelin sheath associated with these large fibers ranged from 0.12 to  $0.4 \mu\text{m}$  thick.

## DISCUSSION

In the present experimental work we have studied the direct projection from the parafoveal regions of V1 to V5 with the view of establishing a structural basis for the transmission of the component motion signal from V1 to V5. The source of the V1 afferents is known to be the spiny stellates and pyramidal cells of layer 4B and large pyramidal cells (Meynert cells) of layer 6

(Lund et al., 1975; Fries et al., 1985; Shipp and Zeki, 1989; Elston and Rosa, 1997). These neurons formed asymmetric (Gray's type 1) synapses with their targets. Nearly 80% of the synaptic targets of V1 afferents in V5 were the spines and dendritic shafts of excitatory cells. The remaining synapses were with the dendrites and somata of smooth (GABAergic inhibitory) neurons.

The similarity between the thalamic and feedforward intracortical pathways has been noted by Johnson and Burkhalter (1996) in their comprehensive study of feedforward and feedback connections in the rat visual cortex. Both the thalamic afferent projection in the primate and the V1 to V5 projection have similar terminal laminae and have spiny neurons as their major target. Compared with the projection from V1 to V5, the projections from V1 to lateral extrastriate cortex in the rat show some minor variations in the cells of origin and in the laminar distribution of the terminals. However, the types and proportions of synaptic targets are quite comparable to those found here, with pyramidal cells forming 90% of the targets and GABAergic interneurons the remainder (Johnson and Burkhalter, 1996). Comparable distributions were also found for the projection from the area 17–18 border to the posterior lateral suprasylvian visual area in the cat (Lowenstein and Somogyi, 1991). This suggests a conservation of function of the interareal feedforward projections in mammalian visual cortex. The commissural and “feedback” connections differ in that a much smaller proportion ( $\sim 2\text{--}4\%$ ) of synapses is formed with smooth neurons (Jones and Powell, 1970; Czeiger and White, 1993; Johnson and Burkhalter, 1996).

The injection sites in V1 included all layers, so it is very likely that the sample of boutons included those originating from both the large pyramidal cells (solitary cells of Meynert) on the border between layers 5 and 6 in monkey V1 and the layer 4B neurons. The layer 5/6 Meynert cells are outnumbered by the layer 4B neurons that project to V5 by  $\sim 10:1$  (Maunsell and Van Essen, 1983; Shipp and Zeki, 1989). Although the terminal arborizations of these two neuronal types have yet to be distinguished, the marked differences in the numbers of these two types that project to V5 suggest that most of the terminals we sampled would have originated from the 4B neurons. Qualitatively, however, we did not get any hint that we might be sampling from two quite distinct populations, at least in terms of their morphology and synaptic targets, and we have therefore treated the V5 population as one homogenous sample. The appearance of anatomical homogeneity may reflect the physiological homogeneity seen by Movshon and Newsome (1996). Six of the neurons they recorded were from layer 4B, and six were from the layer 5/6 border, i.e., probably Meynert cells. All 12 had similar receptive field properties, including strong contrast-independent direction selectivity, and all had fast-conducting axons. This relation of projection pattern to physiology led Movshon and Newsome (1996) to follow Zeki (1974) and characterize V1 as a vast “clearing house” that selectively distributes different specific information to different visual areas.

←

those of neurons with smooth dendrites, which contain GABA. In subsequent sections of the series, the same labeled bouton formed another two synapses with the dendrite. The spine target is almost completely enveloped by the bouton. The extensive postsynaptic density within the spine indicates that the synapse has been sectioned at an oblique plane. *B*, Large bouton located in layer 6 with a dendritic target similar to the one described above (Fig. 3A). The labeled bouton forms an asymmetric synapse (*large, solid arrowhead*) with the dendrite, which also forms symmetric synapses (*open arrowheads*), and other asymmetric synapses (*small, solid arrowheads*) from unidentified boutons. *C*, A higher-power micrograph of the adjacent section in the series of the bouton shown in Figure 3B. Detail of the unlabeled symmetric synapse (*open arrowhead*) and the labeled and unlabeled asymmetric synapses (*large, solid* and *small, solid arrowheads*, respectively) can be compared. Scale bars: *A*, *B*,  $1 \mu\text{m}$ ; *C*,  $0.5 \mu\text{m}$ .

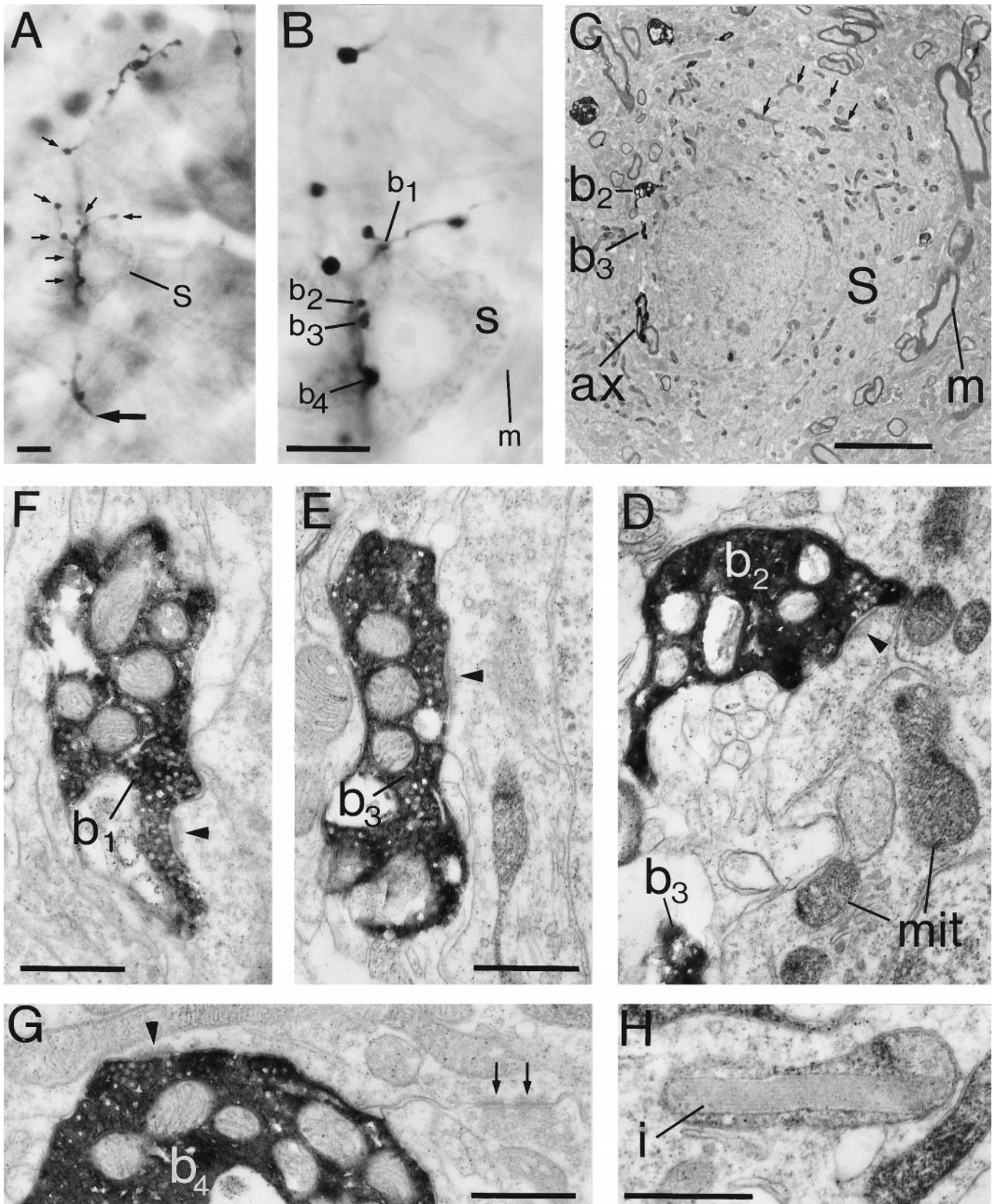


**Figure 5.** Correlated light and electron micrographs of BDA/PHA-L-filled boutons in synaptic contact with a soma (*S*) located in layer 4 of area V5. *A*, Low-power light micrograph of an identified axon collateral (*large, solid arrow*) rising through lower layer 4. The soma (*S*) and some of the boutons (*small arrows*) appear at higher magnification in *B*. *B*, Numbered boutons (*b1*, *b2*, *b3*, *b4*) all form contacts with the soma (*S*). A large-diameter myelinated axon (*m*) is indicated for reference. *C*, Low-power electron micrograph of the soma (*S*) seen in *B*. The myelinated axon (*m*) referred to in *B* can be seen in close contact with the soma. Some of the mitochondria appear to be lightly stained (*small arrows*) (*Figure legend continues*),

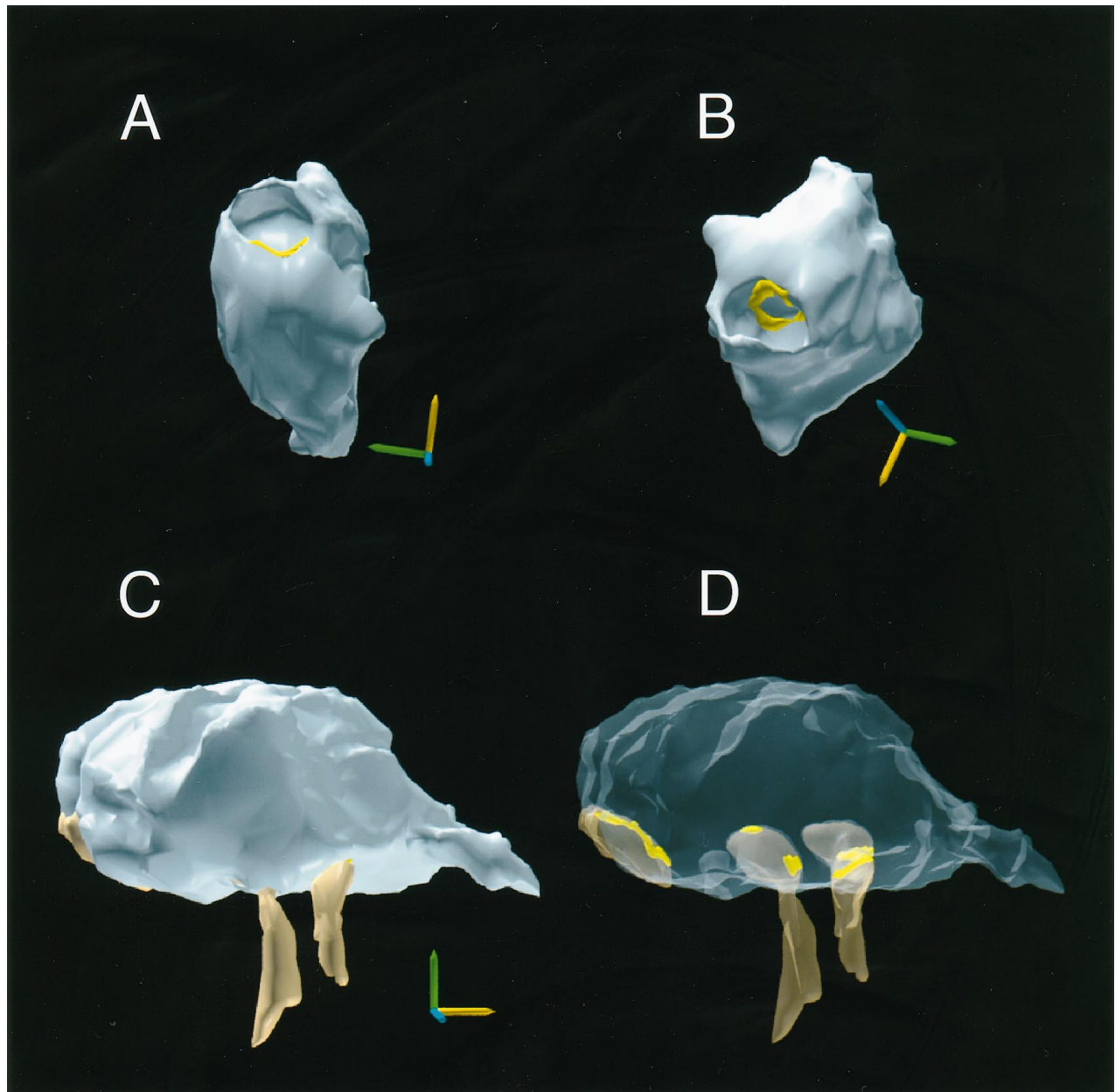


**Figure 6.** Three-dimensional reconstructions from serial ultrathin sections of filled boutons in area V5 showing how targets are enveloped by the bouton. *A, B*, Two views of a bouton (blue) found in layer 6. In *A* a clear depression or pocket can be seen at the top (uppermost pole) of the bouton. The edge of the postsynaptic density (yellow) can be seen at the lip of the depression. In *B* the bouton was rotated around a vertical axis ( $\sim 180^\circ$ ) to provide a better view of the postsynaptic density. *C, D*, A large layer 6 bouton (blue) that forms synapses with three spines (brown). In *C* the bouton and spines have an opaque skin, and in *D* the skin is transparent. The two spines on the right are deeply embedded within the bouton. The postsynaptic surface (yellow) is shown in apposition with the spines. Axes,  $0.5 \mu\text{m}$ .

#### Identification of target neurons and likely synaptic efficacy

The pyramidal cells in V5 are more highly branched and more spiny than those of V1 pyramidal cells (Elston and Rosa, 1997).

This is perhaps a consequence of the higher density of neurons in V1 that may prevent elaboration of the dendritic tree. The number of excitatory synapses formed on these V5 pyramidal cells is probably in the range of 5000 to 10,000, as in other cortical areas.

←

thus enabling the soma to be seen at the light microscopic level. The large filled axon (*ax*) gives rise to the boutons (*b2, b3*) after losing its myelin sheath (not illustrated). *D*, High-power electron micrograph of boutons *b2* and *b3*. The bouton *b2* forms an asymmetric synapse (solid arrowhead) with the soma. Electron dense mitochondria (*mit*) can be seen within the cytoplasm of the soma. *E, F*, In sections after that shown in *D*, boutons *b3* and *b1* can be seen to form asymmetric synapses (solid arrowheads) with the soma. *G*, The asymmetric synapse (solid arrowhead) of the fourth bouton (*b4*) in contact with the soma can be compared with the asymmetric synapses (small arrows) formed by an unlabeled bouton also in contact with the soma. *H*, High-power micrograph of a crystalline inclusion (*i*) within the body of a mitochondria found in the soma contacted by the above boutons. Scale bars: *A, B*,  $10 \mu\text{m}$ ; *C, 5 \mu\text{m}; *D–H*,  $0.5 \mu\text{m}$ .*

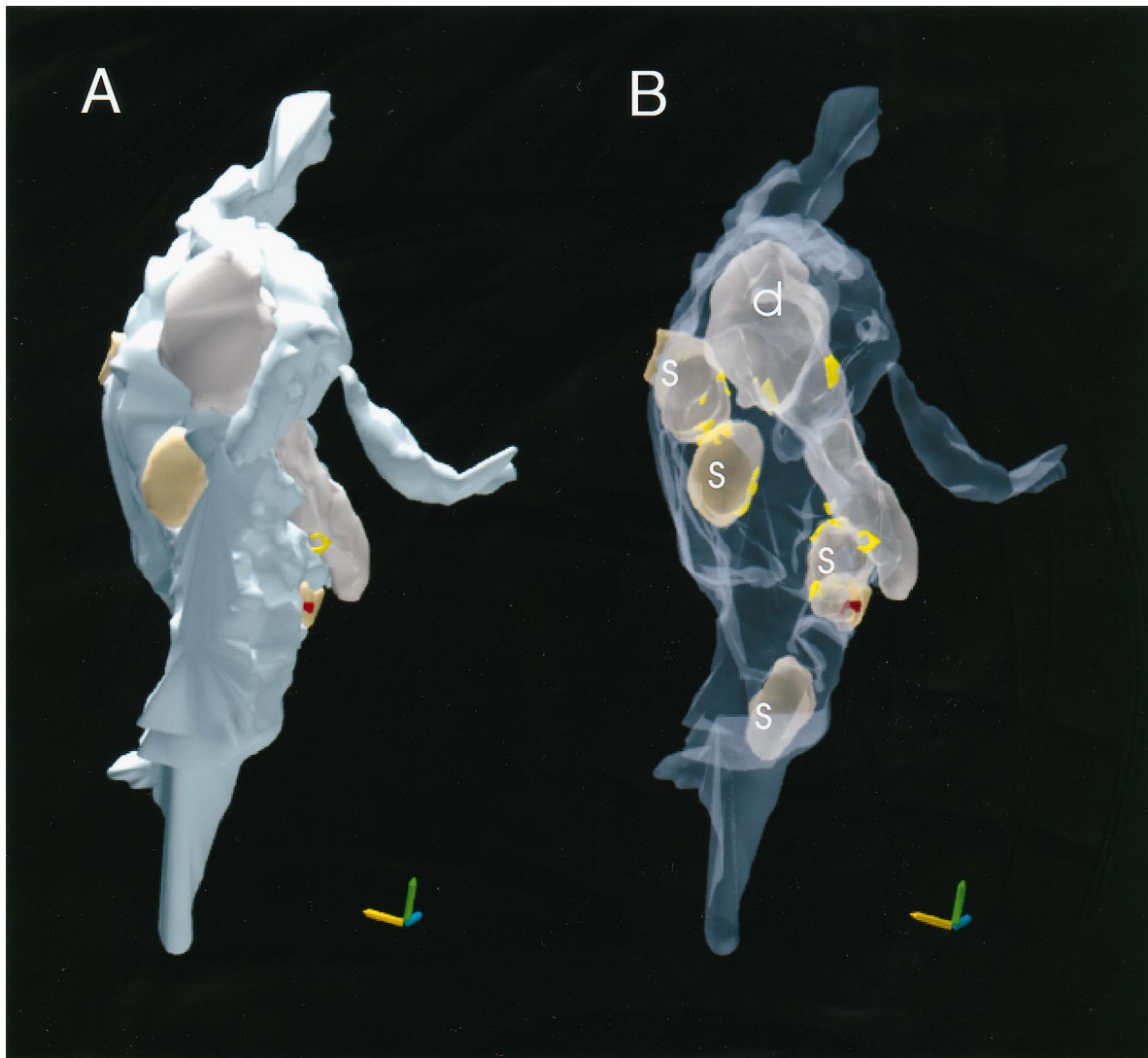


**Figure 7.** Reconstruction of a large bouton (blue) in layer 4 of area V5 that forms synapses with four spines and a dendrite. *A*, When the bouton is rendered with an opaque skin it can be seen to wrap around the dendrite (*d* in *B*). This dendrite forms three synapses with the identified bouton. The spines (*s* in *B*) are all deeply embedded in the bouton. *B*, Both bouton and targets are rendered transparent, showing the postsynaptic density. The asymmetric synapses are yellow. One of the spines also forms a symmetric synapse (red) with an unidentified bouton. Axes,  $0.5 \mu\text{m}$ .

For the basket cells the number is probably similar (Ahmed et al., 1997). Our estimates clearly suggest that the afferents of V1 can only provide a few percent of these excitatory synapses. The unbiased method of counting (Sterio, 1984) makes it likely that we have correctly assessed the percentage of labeled synapses in layer 4 of V5. However, there are possible technical issues that would lead to an underestimate of the actual number. One obvious issue is that not all of the projecting neurons at the site of injection might have taken up and transported the label, or that the transport is incomplete. A more significant issue concerns the divergence and convergence of the V1 to V5 projection. If a single region of V5 receives its input from a very large region of V1, our injections in V1 would have failed to label all of the neurons projecting to the sampled terminal region in V5. However, if not all of the boutons were labeled, this estimate cannot be greatly in error, given that the V5 projection neurons in V1 are sparse and have to map retinotopically in V5. It is likely that each target neuron in V5 must form at most only a few hundred synapses with V1 afferents. This raises the

interesting functional problem for the computation of pattern motion. If V1 does form the first stage of the motion computation and V5 the second, then the signal is being conveyed from V1 to V5 by a small fraction of the synapses. How then does the V1 signal avoid being swamped or corrupted by the activity of all of the other excitatory synapses simultaneously active on the dendritic tree of the recipient V5 neuron?

One possible answer to this question is that the V1 afferent synapses are particularly powerful relative to the other excitatory synapses formed with the V5 neurons. The size of the synaptic potentials in V5 neurons has yet to be measured. However, the size of the postsynaptic densities of the V1 afferent synapses may provide an approximate indication of the number of receptors that could be located in the postsynaptic membrane of the V5 recipient neurons. For example, 1000 AMPA receptors of  $10 \text{ nm}$  diameter could be packed side by side into  $0.1 \mu\text{m}^2$ . Our measurements of the area of the postsynaptic densities of the synapses formed by the labeled boutons indicate that the largest (those on spines) are slightly smaller ( $0.13 \mu\text{m}^2$ ) than those of the thalamo-

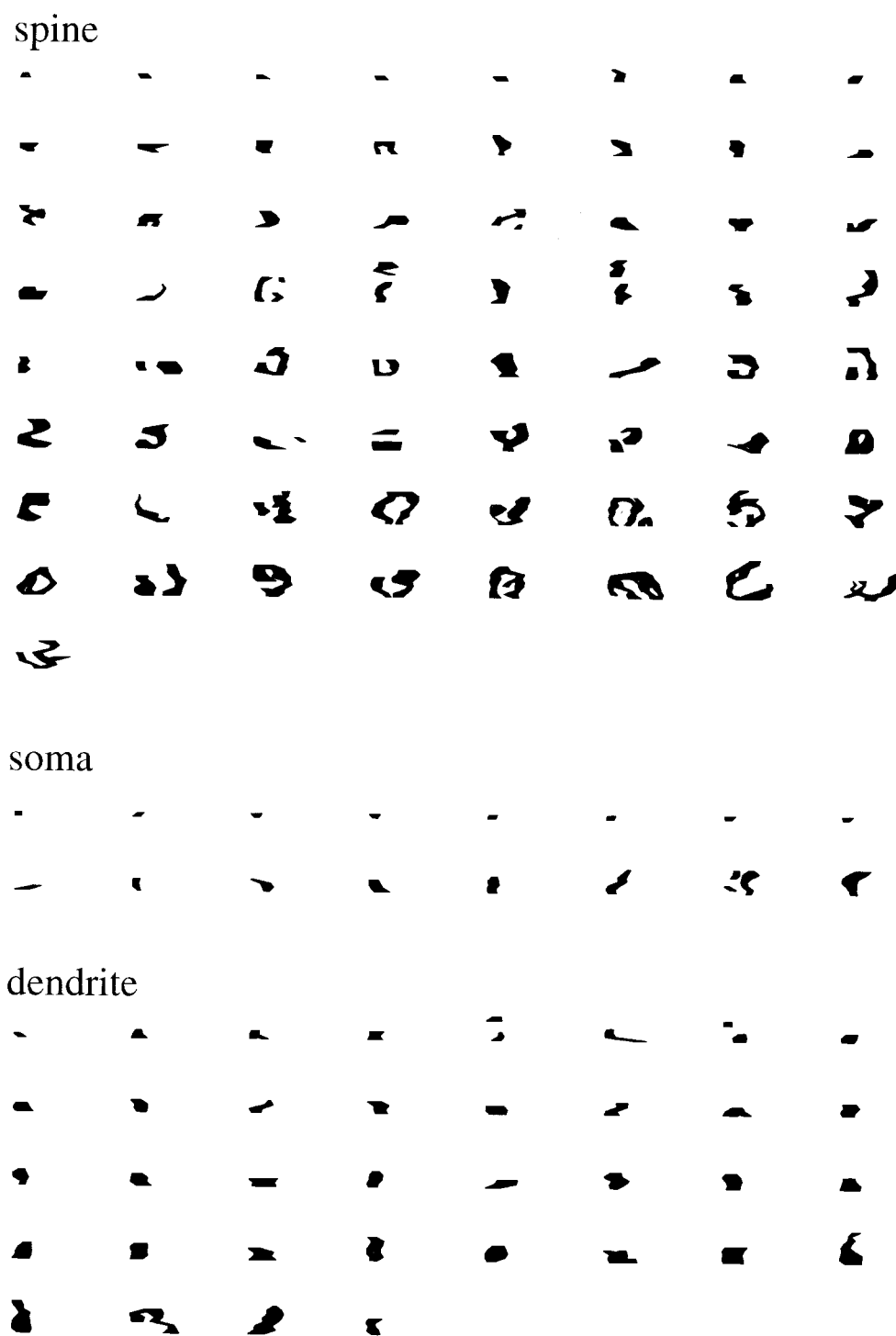


**Figure 8.** Two-dimensional projection of the reconstructed postsynaptic densities found on spines, soma, and dendrites postsynaptic to labeled boutons in area V5. The densities are from individual synapses and are ordered by increasing surface area calculated from the 3-D reconstructions. Scale bar, 1  $\mu\text{m}$ .

cortical synapses in the cat, which are  $\sim 0.18 \mu\text{m}^2$  (Dehay et al., 1991; Friedlander et al., 1991). These postsynaptic densities in V5 are at least threefold larger in area than those observed at comparable excitatory synapses formed with spines of CA1 pyramidal cells in the mouse and rat hippocampus (Harris and

Stevens, 1989; Schikorski and Stevens, 1997). They are slightly smaller than the individual synapses formed by single mossy fiber boutons with the branched dendritic spines of the CA3 pyramids (Chicurel and Harris, 1992).

Individual geniculocortical fibers in the cat visual cortex pro-

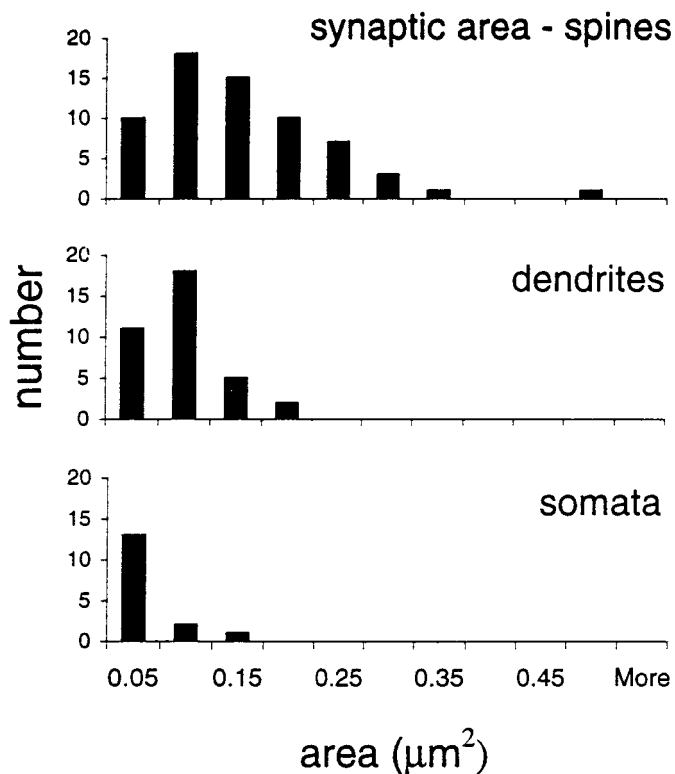


Figure 9. Histogram of the distribution of postsynaptic areas ( $\mu\text{m}^2$ ) formed by labeled boutons in area V5.

vide average EPSP amplitudes of nearly 2 mV, which would require >400 postsynaptic ion channel openings (Stratford et al., 1996). The extraordinarily low coefficient of variation of 8% suggests that they could arise from multiple release sites with an extremely high release probability or single large synapses (Stratford et al., 1996). By analogy with these cat data, the size of the V5 synapses studied here suggest that the mean amplitudes of the unitary AMPA receptor EPSPs will be  $\sim 1$ –2 mV. This remains to be tested. We also found evidence of multisynaptic connections from single afferents to single neurons in V5. Unfortunately, our method cannot provide an estimate of the frequency of such multisynaptic connections, but such multiple synapses would lead to larger EPSPs and so provide V5 with a functionally powerful input from V1 despite the small number of synapses that the V1 projection provides in V5.

#### Influence of synapse morphology on transmitter diffusion

The 3-D reconstruction of the postsynaptic elements revealed that the postsynaptic densities formed with dendritic shafts were single disks. By contrast the synapses formed with spines had perforated postsynaptic densities that formed complex horseshoe or circular arrangements when viewed *en face*. In addition, the larger presynaptic boutons enveloped the entire head of the postsynaptic spines and occasionally dendritic shafts. We do not yet understand why the spine synapses in the V1 to V5 projection form such elaborate morphology, but presumably one reason is to secure more efficient and reliable transmission with the fewest possible synapses. Previously we have observed such embedding of the postsynaptic target in the presynaptic bouton in the magnocellular boutons of the thalamic afferents in V1 of the macaque

monkey (Freund et al., 1989) and in boutons of the nondeprived Y-axons in area 18 of long-term monocularly deprived cats (Friedlander et al., 1991). Elsewhere, the giant mossy fiber boutons in CA3 of the hippocampus also appear to embed their targets (Chicurel and Harris, 1992). An additional feature of such large boutons is that they form multiple synapses. Such arrangements could have some significance for the spillover of neurotransmitter between receptor domains within a single postsynaptic or perisynaptic complex and for spread of transmitter between synapses.

The diffusion of glutamate neurotransmitter from the synapse has been modeled in some detail (Uteshev and Pennefather, 1997; Rusakov and Kullmann, 1998a,b). Kullman and Asztely (1998) have reviewed the relevant experimental literature. The modeling shows that both the viscosity (determined by the diffusing molecules interactions with cell walls and macromolecules in the extracellular space) and geometry of the tissue have a significant effect on diffusion. Rusakov and Kullman (1998a) show that NMDA receptors, but not AMPA receptors, located at a distance of  $\sim 500$  nm from the center of the synaptic cleft will be activated by the release of one vesicle. The synapses formed by the multisynaptic boutons in V5 tended to have intersynaptic distances in excess of 500 nm. This, together with the envelopment of the synapses by the bouton, would restrict the cross-talk between these synapses. However, this same morphology might increase the concentration of neurotransmitter in the region surrounding the synapse and so increase the probability of the activation of receptors on both the postsynaptic and the presynaptic membrane. The “gap” between the synaptic densities in the perforated synapses averaged  $\sim 300$  nm (range, 168 to 476 nm) (Fig. 8), which is within the effective diffusion range of the contents of a single vesicle (Rusakov and Kullman, 1998a). The same constraints of diffusion studied by Rusakov and Kullman (1998a,b) of course applies to the movement of extracellular ions, such as  $\text{Ca}^{2+}$ , into the boutons. If the diffusion of  $\text{Ca}^{2+}$  is slow, then it may become locally depleted and so modify synaptic activity (Montague, 1996).

Little attention has been paid to the correlation between synaptic morphology and physiology in the visual cortex. Nevertheless, there are some quite distinct differences in the synaptic physiology of the inputs to layer 4 of cat visual cortex, as noted above. In particular the thalamocortical synapses in the cat produce EPSPs of large amplitude and exceedingly low variance (Stratford et al., 1996). This is most easily explained if only a single release site were active. However, the contents of a single vesicle [ $\sim 5000$  molecules of neurotransmitter (Riveros et al., 1986)] may not contain enough transmitter to produce 100% double occupancy (saturation) of the receptors that such low variance implies (Larkman et al., 1991). Thus, multiple release sites, each having a high probability of release, may invariably be involved in such synapses if the diffusion distance between any single release site and target receptors is to be reduced.

Synapses with multiple release sites that have large-amplitude low-variance synaptic currents have been observed in the multi-site glutamatergic synapses that mossy fibers form with granule cells in the rat's cerebellum (Silver et al., 1996). At these sites the synaptic current appears to be limited by the number of postsynaptic channels rather than by the amount of neurotransmitter released. This is probably because the transmitter released from neighboring sites overlaps and so changes both the concentration and length of occupancy of the transmitter in the cleft (Faber and Korn, 1988). Importantly too, the perisynaptic concentration of

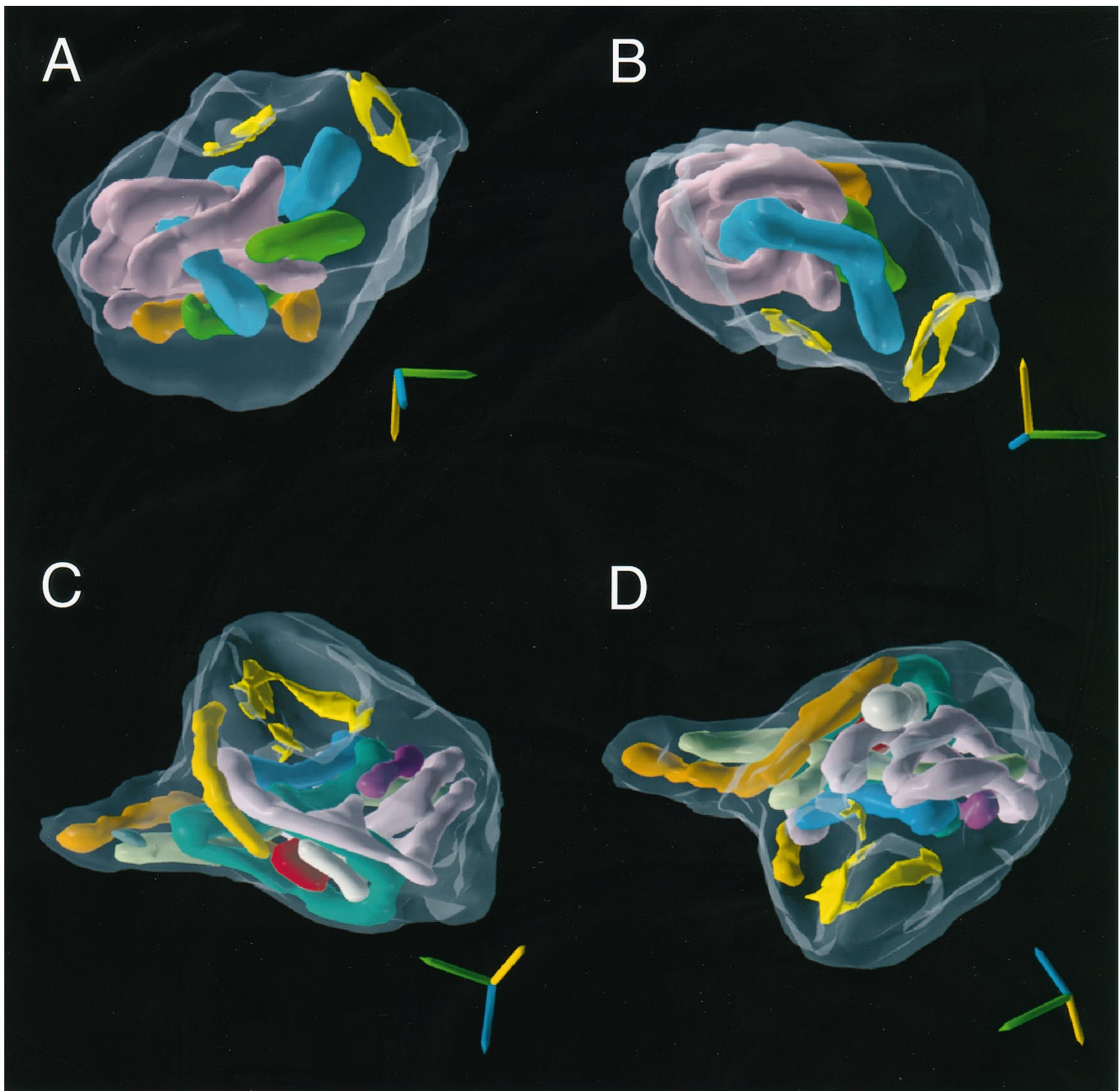


**Figure 10.** Two different views of two boutons reconstructed and rendered with transparent skins to show solid mitochondria and postsynaptic specializations (yellow). The mitochondria are color-coded for identification of individual structures. For both boutons the right-hand image (*B, D*) is rotated ( $\sim 180^\circ$ ) about the horizontal axis of the left-hand image. *A, B*, Bouton found in layer 6 that formed synapses with two spines and contained four mitochondria (pink, blue, orange, and green). The longest mitochondrion (pink) was branched and formed three loops. Both synaptic surfaces (yellow) are presented at oblique, nonoptimal elevations but appear as incomplete annuli. *C, D*, Layer 4 bouton formed synapses with two spines and contained nine mitochondria. One mitochondrion (pink) is branched and forms loops. The synaptic specializations (yellow) become superimposed on each other in these views. One synapse is horseshoe-shaped and the second is composed of two small patches. Axes,  $0.5 \mu\text{m}$ .

transmitters would also be raised. One possibility is that there are receptors located in the perforation of the postsynaptic density—for example, the metabotropic glutamate receptors (Nusser et al., 1994; Baude et al., 1995). Extrasynaptic receptors located at the center of the horseshoe would be at a relative advantage because they would receive a higher concentration of spillover neurotransmitter from multiple release sites than receptors located outside the ring. Unfortunately the neurochemistry and distribution of V5 receptors is unknown.

The smallest postsynaptic densities seen in the present study were formed mainly with dendritic shafts. In the cat, the smallest postsynaptic densities are also on the dendritic shafts, but their source is local layer 6 pyramidal cells. (Ahmed et al., 1994, 1997). These layer 6 pyramidal cell synapses show strong paired-pulse facilitation and not the paired-pulse depression seen with the layer 4 spiny stellate synapses or the thalamic afferent synapses (Stratford et al., 1996; Tarczy-Hornoch et al., 1998). The mechanisms that determine this dynamic behavior of synapses are

### Targets of V1 boutons in area MT



Figure 11. Histogram of synaptic targets of boutons in area V5 originating from neurons labeled in area V1.

### synapses per bouton

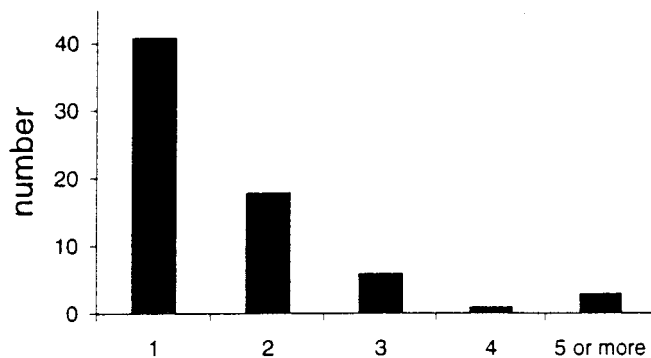


Figure 12. Histogram of the number of synapses (1, 2, 3, 4, or more per bouton) formed by individual labeled boutons in layers 4 and 6 of area V5.

largely unknown. However, it has recently been discovered that the mitochondria may have an important role in the dynamics of synaptic function.

#### Mitochondria in the synaptic boutons

A striking morphological feature was the considerable volume occupied by mitochondria within the terminal boutons of the V1 afferent neurons. In a previous study in the cat it was noted that the number of mitochondrial profiles seen in a single cross section of a thalamic afferent bouton scaled linearly with the size of the bouton (Friedlander et al., 1991). By making the 3-D reconstructions, it became clear that the many mitochondrial profiles seen in a single cross section actually arose from the tortuous folding and branching of individual mitochondria within the bouton. The functional role of the mitochondria in the presynaptic terminals is beginning to be understood from work in invertebrates and lower vertebrates. In the crayfish, the axon terminals of phasic motoneurons contain fewer mitochondria and show marked synaptic depression, whereas the terminals of tonic motoneurons have more mitochondria, more oxidative activity, and a greater resistance to synaptic depression. The synapses of the tonic motoneurons also show strong frequency-dependent facilitation (Nguyen et al., 1997). These data suggest the possibility that the V1 neurons projecting to MT have a tonic activity and that one role of the mitochondria in the boutons is to prevent or reduce depression in this synapse.

Mitochondria play an important role in calcium metabolism in cells (Nicholls and Åkerman, 1982; Herrington et al., 1996; Xu et al., 1997), but despite the importance of calcium in synaptic

### Area ( $\mu\text{m}^2$ ) of labeled and non-labeled boutons in area V5

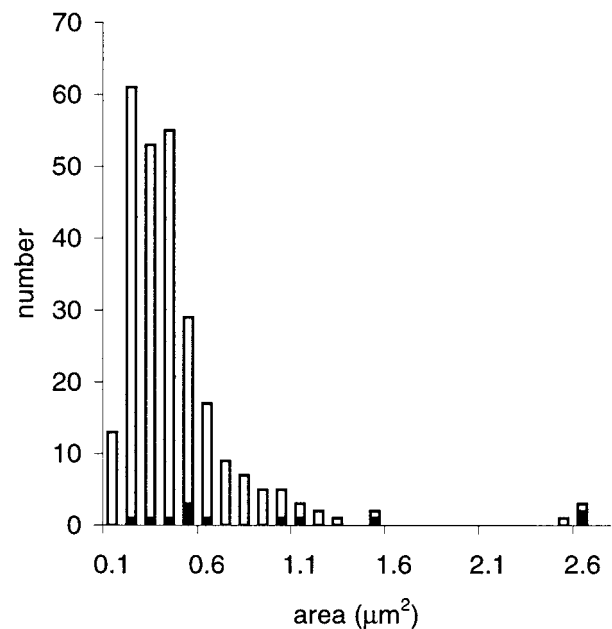


Figure 13. Histogram showing the distribution of area ( $\mu\text{m}^2$ ) of labeled (black bars) and nonlabeled (white bars) synaptic boutons in area V5. Only those boutons with disappearing synapses were measured.

transmission, the significance of mitochondria for synaptic transmission has only recently been recognized. Calcium enters the synaptic bouton through voltage-gated channels, and it is the key ion in producing the release of neurotransmitter. Increasing the calcium concentration within the bouton increases the probability of transmitter release. In the bullfrog sympathetic ganglia (Peng, 1998), calcium entering the bouton is taken up by the mitochondria, but in a frequency-dependent manner. If the terminal is activated at low rates, then the calcium transporters in the mitochondria can provide adequate buffering. If the rates of activation are high, the mitochondria cannot buffer adequately, and calcium accumulates within the bouton. This uptake during repetitive stimulation also explains the development of post-tetanic potentiation at synapses. Tang and Zucker (1997) have found that mitochondria in the neuromuscular junction of the crayfish also slowly release the calcium they accumulated during tetanic stimulation. It is this maintained higher concentration of calcium within the bouton that is responsible for post-tetanic potentiation.

Although the role of mitochondria at central synapses in mammals has still to be studied, it is most likely that their role in the boutons studied here includes the mechanisms referred to in the above studies of invertebrate and lower vertebrate synapses. Thus, the quantification of the contribution of mitochondria within the synaptic boutons of identified neurons may provide another important link between morphology and function of these synapses.

#### Common basic circuits in V1 and V5

On anatomical grounds, therefore, it seems that both the light and electron microscopic pattern of innervation of the V1 afferents in V5 does not differ markedly from that of the dLGN input to V1. Johnson and Burkhalter (1996) have suggested schemes of how the thalamic and interareal feedforward and feedback circuits

might connect into the local recurrent microcircuits of the visual cortex (Douglas et al., 1989a,b). Models of component direction selectivity have been simulated on such recurrent microcircuits (Douglas and Martin, 1991; Suarez et al., 1995). In principal, the extraction of global motion should be possible using the same machinery as is used for the component motion analysis. Simoncelli and Heeger (1998) have developed an abstract linear model to explain how global motion in V5 can be derived from a component motion input from V1 by means of essentially the same algorithm. Although their model does not map directly onto the known circuitry and biophysics of the cortex, they pointed out that the commonality of their computation for V1 and V5 is conceptually related to the structural commonality of circuits in different cortical areas. It is this same principle of multifunctionality of a basic circuit that is captured in the concept of the recurrent microcircuit (Douglas et al., 1989a,b; Douglas and Martin, 1991).

### Future prospects

The present study has raised some important questions about the possible role of the V1 input to V5. Obviously, V5 receives other inputs from areas such as V2, V3, VP, MST, and the thalamus. Blocking all of the activity transmitted from V1 either by cooling appropriate retinotopic regions (Girard et al., 1992) or by ablation (Rodman et al., 1990) leaves V5 quite impaired but still partly functional. The remaining active neurons are directional. Combined lesions of the colliculus and V1 eliminate activity in V5 (Rodman et al., 1990). These alternative routes are not evidence against the hypothesis of Movshon and Newsome (1996) that the computation of pattern motion takes place in V5. However, considerable work still needs to be done to settle the matter. Clearly, in view of the results obtained in this study, it will be important to establish whether V5 is built of recurrent circuits comparable in structure and function to those of V1.

### REFERENCES

- Adelson EH, Movshon JA (1982) Phenomenal coherence of moving visual patterns. *Nature* 300:523–525.
- Ahmed B, Anderson JC, Martin KAC, Nelson JC (1994) Polyneuronal innervation of spiny stellate neurons in cat visual cortex. *J Comp Neurol* 341:39–49.
- Ahmed B, Anderson JC, Martin KAC, Nelson JC (1997) Map of the synapses onto layer 4 basket cells of the primary visual cortex of the cat. *J Comp Neurol* 380:230–242.
- Allman JM, Kaas JH (1971) A representation of the visual field in the caudal third of the middle temporal gyrus of the owl monkey (*Aotus trivirgatus*). *Brain Res* 31:85–105.
- Baude A, Nusser Z, Molnár E, McIlhenny RAJ, Somogyi P (1995) High-resolution immunogold localization of AMPA type glutamate receptor subunits at synaptic and non-synaptic sites in rat hippocampus. *Neuroscience* 69:1031–1055.
- Chan-Palay V, Palay SL, Billings-Gagliardi SM (1974) Meynert cells in the primate visual cortex. *J Neurocytol* 3:631–658.
- Chicurel ME, Harris KM (1992) Three-dimensional analysis of the structure and composition of CA3 branched dendritic spines and their synaptic relationships with mossy fiber boutons in the rat hippocampus. *J Comp Neurol* 325:169–182.
- Colonnier M (1968) Synaptic patterns of different cell types in the different laminae of the cat visual cortex: an electron microscopic study. *Brain Res* 9:268–287.
- Czeiger D, White EL (1993) Synapses of extrinsic and intrinsic origin made by callosal projection neurons in mouse visual cortex. *J Comp Neurol* 330:502–513.
- Dehay C, Douglas RJ, Martin KAC, Nelson JC (1991) Excitation by geniculocortical synapses is not “vetoed” at the level of dendritic spines in cat visual cortex. *J Physiol (Lond)* 440:723–734.
- Douglas RJ, Martin KAC (1991) A functional microcircuit for cat visual cortex. *J Physiol (Lond)* 440:735–769.
- Douglas RJ, Martin KAC, Whitteridge D (1989a) A canonical microcircuit for neocortex. *Neural Comput* 1:480–488.
- Douglas RJ, Martin KAC, Whitteridge D (1989b) A functional microcircuit for cat visual cortex. *J Physiol (Lond)* 440:735–769.
- Dubner R, Zeki S (1971) Response properties and receptive fields in an anatomically defined region of the superior temporal sulcus in the monkey. *Brain Res* 35:528–532.
- Elston GN, Rosa GP (1997) The occipitoparietal pathway of the macaque monkey: comparison of pyramidal cell morphology in layer 3 of functionally related cortical visual areas. *Cereb Cortex* 7:432–452.
- Faber DS, Korn H (1988) Synergism at central synapses due to lateral diffusion of transmitter. *Proc Natl Acad Sci USA* 85:8708–8712.
- Freund TF, Martin KAC, Soltesz I, Somogyi P, Whitteridge D (1989) Arborisation pattern and postsynaptic targets of physiologically identified thalamocortical afferents in striate cortex of the macaque monkey. *J Comp Neurol* 289:315–336.
- Friedlander MJ, Martin KAC, Wassenhove-McCarthy D (1991) Effects of monocular visual deprivation on the innervation of cortical area 18 in the cat by individual thalamocortical axons. *J Neurosci* 11:3268–3288.
- Fries W, Keizer K, Kuypers HG (1985) Large layer VI cells in macaque striate cortex (Meynert cells) project to both superior colliculus and prestriate visual area V5. *Exp Brain Res* 58:613–616.
- Gilbert CD (1977) Laminar differences in receptive field properties of cells in cat primary visual cortex. *J Physiol (Lond)* 268:391–421.
- Girard P, Salin PA, Bullier J (1992) Response selectivity of neurons in area MT of the macaque monkey during reversible inactivation of area V1. *J Neurophysiol* 67:1437–1446.
- Gray EG (1959) Axosomatic and axodendritic synapses in the cerebral cortex: an electron microscopic study. *J Anat* 93:420–433.
- Harris KM, Stevens JK (1989) Dendritic spines of CA1 pyramidal cells in the rat hippocampus: serial electron microscopy with reference to their biophysical characteristics. *J Neurosci* 9:2982–2997.
- Herrington J, Park YB, Babcock DF, Hille B (1996) Dominant role of mitochondria in clearance of large Ca<sup>2+</sup> loads from rat adrenal chromaffin cells. *Neuron* 16:219–228.
- Johnson RR, Burkhalter A (1996) Microcircuitry of forward and feedback connections within rat visual cortex. *J Comp Neurol* 368:383–398.
- Jones EG, Powell TPS (1970) An electron microscope study of the laminar pattern and mode of termination of afferent fibre pathways in the somatic sensory cortex of the cat. *Philos Trans R Soc Lond B Biol Sci* 257:45–62.
- Kisvárdy ZF, Martin KAC, Whitteridge D, Somogyi P (1985) Synaptic connections of intracellularly filled clutch neurons, a type of small basket neuron in the visual cortex of the cat. *J Comp Neurol* 241:111–137.
- Kullmann DM, Asztely F (1998) Extrasynaptic glutamate spillover in the hippocampus: evidence and implications. *Trends Neurosci* 21:8–14.
- Larkman A, Stratford KJ, Jack JJB (1991) Quantal analysis of excitatory synaptic action and depression in hippocampal slices. *Nature* 350:344–347.
- LeVay S (1986) Synaptic organization of claustral and geniculate afferents to the visual cortex of the cat. *J Neurosci* 6:3564–3575.
- Lowenstein PR, Somogyi P (1991) Synaptic organization of cortico-cortical connections from the primary visual cortex to the posteromedial lateral suprasylvian visual area in the cat. *J Comp Neurol* 310:253–266.
- Lund JS, Lund RD, Hendrickson AE, Bunt AH, Fuchs AF (1975) The origin of efferent pathways from the primary visual cortex, area 17, of the macaque monkey as shown by retrograde transport of horseradish peroxidase. *J Comp Neurol* 164:287–303.
- Maunsell JH, Van Essen DC (1983) The connections of the middle temporal visual area (MT) and their relationship to a hierarchy in the macaque. *J Neurosci* 3:2563–2586.
- Montague PR (1996) The resource consumption principle: attention and memory in volumes of neural tissue. *Proc Natl Acad Sci USA* 93:3619–3623.
- Movshon JA, Newsome WT (1984) Functional characteristics of functional cortical neurons projecting to MT in the macaque. *Soc Neurosci Abstr* 10:933.
- Movshon JA, Newsome WT (1996) Visual response properties of striate cortical neurons projecting to area MT in macaque monkeys. *J Neurosci* 16:7733–7741.
- Nguyen PV, Marin L, Atwood HL (1997) Synaptic physiology and mi-

- tochondrial function in crayfish tonic and phasic motor neurons. *J Neurophysiol* 78:281–294.
- Nicholls DG, Åkerman KEO (1982) Mitochondrial calcium transport. *Biochim Biophys Acta* 683:57–88.
- Nusser Z, Mulvihill E, Streit P, Somogyi P (1994) Subsynaptic segregation of metabotropic and ionotropic glutamate receptors as revealed by immunogold localization. *Neuroscience* 61:421–427.
- Palmer LA, Rosenquist AC (1974) Visual receptive fields of single striate cortical units projecting to the superior colliculus in the cat. *Brain Res* 67:27–42.
- Peng Y-Y (1998) Effects of mitochondrion on calcium transients at intact presynaptic terminals depend on frequency of nerve firing. *J Neurophysiol* 80:186–195.
- Peters A, Saint Marie RL (1984) Smooth and sparsely spinous non-pyramidal cells forming local axonal plexuses. In: *Cerebral cortex*, Vol 1. Cellular components of the cerebral cortex (Jones EG, Peters A, eds), pp 419–445. New York: Plenum.
- Peters A, Palay SL, Webster HDeF (1991) *The fine structure of the nervous system: neurons and their supporting cells*, Ed 3. Oxford, UK: OUP.
- Riveros N, Fieldler J, Lagos N, Munoz C, Orrego G (1986) Glutamate in rat brain cortex synaptic vesicles: influence of the vesicle isolation procedure. *Brain Res* 386:405–408.
- Rockland KS (1989) Bistratified distribution of terminal arbors of individual axons projecting from area V1 to middle temporal area (MT) in the macaque monkey. *Vis Neurosci* 3:155–170.
- Rockland KS (1995) Morphology of individual axons projecting from area V2 to MT in the macaque. *J Comp Neurol* 355:15–26.
- Rodman HR, Gross CG, Albright TD (1990) Afferent basis of visual response properties in area MT of the macaque. II. Effects of superior colliculus removal. *J Neurosci* 10:1154–1164.
- Rusakov DA, Kullman DM (1998a) Extrasynaptic glutamate diffusion in the hippocampus: ultrastructural constraints, uptake, and receptor activation. *J Neurosci* 18:3158–3170.
- Rusakov DA, Kullman DM (1998b) Geometric and viscous components of the tortuosity of the extracellular space in the brain. *Proc Natl Acad Sci USA* 95:8975–8980.
- Schikorski T, Stevens CF (1997) Quantitative ultrastructural analysis of hippocampal excitatory synapses. *J Neurosci* 17:5858–5867.
- Shipp S, Zeki S (1989) The organisation of connections between area V5 and V1 in macaque monkey visual cortex. *Eur J Neurosci* 1:309–332.
- Silver RA, Cull-Candy SG, Takahashi T (1996) Non-NMDA glutamate receptor occupancy and open probability at a rat cerebellar synapse with single and multiple release sites. *J Physiol (Lond)* 494:231–250.
- Simoncelli EP, Heeger DJ (1998) A model of neuronal responses in visual area MT. *Vision Res* 38:743–761.
- Somogyi P, Kisvárdy ZF, Martin KAC, Whitteridge D (1983) Synaptic connections of morphologically identified and physiologically characterised large basket cells in the striate cortex of cat. *Neuroscience* 10:261–294.
- Sterio DC (1984) The unbiased estimation of number and sizes of arbitrary particles using the disector. *J Microsc* 134:127–136.
- Stratford KJ, Tarczy-Hornoch K, Martin KAC, Bannister NJ, Jack JJB (1996) Excitatory synaptic inputs to spiny stellate cells in cat visual cortex. *Nature* 382:258–261.
- Suarez HH, Koch C, Douglas RJ (1995) Modeling direction selectivity of simple cells in striate visual cortex within the framework of the canonical microcircuit. *J Neurosci* 15:6700–6719.
- Tang Y-G, Zucker RS (1997) Mitochondrial involvement in post-tetanic potentiation of synaptic transmission. *Neuron* 18:483–491.
- Tarczy-Hornoch K, Martin KAC, Jack JJB, Stratford KJ (1998) Synaptic interaction between smooth and spiny neurons in layer 4 of cat visual cortex. *J Physiol (Lond)* 508:351–363.
- Ungerleider LG, Mishkin M (1979) The striate projection zone in the superior temporal sulcus of *Macaca mulatta*: location and topographic organisation. *J Comp Neurol* 188:347–366.
- Uteshev VV, Pennefather PS (1997) Analytical description of the activation of multi-state receptors by continuous neurotransmitter signals at brain synapses. *Biophys J* 72:1127–1134.
- Xu T, Naraghi M, Kang H, Neher E (1997) Kinetic studies of  $Ca^{2+}$  binding and  $Ca^{2+}$  clearance in the cytosol of adrenal chromaffin cells. *Biophys J* 73:532–545.
- Zeki S (1969) Representation of central fields in prestriate cortex of monkey. *Brain Res* 19:63–75.
- Zeki S (1974) Functional organisation of a visual area in the posterior bank of the superior temporal sulcus of the rhesus monkey. *J Physiol (Lond)* 236:549–573.